ity on addition of competing monovalent ligand will confer a degree of flexibility not possible with avidin·biotin.

REFERENCES AND NOTES

1. M. N. Matrosovich, *FEBS Lett.* **252**, 1 (1989).
2. A. Spaltenstein and G. M. Whitesides, *J. Am. Chem. Soc.* **113**, 686 (1991).
3. Y. C. Lee and R. T. Lee, *Acc. Chem. Res.* **28**, 321 (1995).
4. R. Roy and F. D. Tropper, *J. Chem. Soc. Chem. Commun.* **1988**, 1058 (1988).
5. G. B. Sigal, M. Mammen, G. Dahmann, G. M. Whitesides, *J. Am. Chem. Soc.* **118**, 3789 (1996).
6. Divalent interactions involving two linked ligands interacting with two linked receptors have been studied in many systems, including dimers of cyclodextrin with divalent ligands [R. Breslow and B. Zhang, *ibid.*, p. 8495], dimers of sialyl Lewis X with E-selectin [C.-H. Wong *et al.*, *ibid.* **117**, 66 (1995)], dimers of immunophilin ligands such as FK506 and cyclosporin A with receptors active in controlling cellular signal transduction [D. M. Spencer, T. J. Wandless, S. L. Schreiber, G. R. Crabtree, *Science* **262**, 1019 (1993)], and divalent antibodies with surface antigens [C. L. Hornick and F. Karush, *Immunochemistry* **9**, 325 (1972)].
7. J. Rao and G. M. Whitesides, *J. Am. Chem. Soc.* **119**, 10286 (1997).
8. N. M. Green, *Biochem. J.* **89**, 585 (1963).
9. D. H. Williams, *Tetrahedron* **40**, 569 (1984).
10. M. Schafer, T. R. Schneider, G. M. Sheldrick, *Structure* **4**, 1509 (1996).
11. P. J. Loll, A. E. Bevivino, B. D. Korty, P. H. Axelsen, *J. Am. Chem. Soc.* **119**, 1516 (1997).
12. D. H. Williams, *Acc. Chem. Res.* **17**, 364 (1984).
13. A. Cooper and K. E. McAuley-Hecht, *Philos. Trans. R. Soc. London Ser. A* **345**, 23 (1993).
14. M. Nieto and H. R. Perkins, *Biochem. J.* **123**, 773 (1971).
15. P. Groves, M. S. Searle, J. P. Waltho, D. H. Williams, *J. Am. Chem. Soc.* **117**, 7958 (1995).
16. U. Gerhard, J. P. Marckay, R. A. Maplestone, D. H. Williams, *ibid.* **115**, 232 (1993).
17. U. N. Sundram, J. H. Griffin, T. I. Nicas, *ibid.* **118**, 13107 (1996).
18. C. M. Harris and T. M. Harris, *ibid.* **104**, 4293 (1982).
19. U. N. Sundram and J. H. Griffin, *J. Org. Chem.* **60**, 1102 (1995).
20. The R_tV_3 hexatrifluoroacetate was isolated as white foam after lyophilization. The ^{1}H-NMR spectrum showed the resonances expected for the central aromatic spacer {400 MHz, dry dimethyl-d_6 sulfoxide, δ [parts per million (ppm)] relative to tetramethylsilane (TMS): 4.45 (d, CH_2NH), 7.28 (d, ArH), 7.74 (d, ArH), 8.70 (s, ArH), 10.60 (s, CONH)}and vancomycin units. The ESIMS exhibited an ion at a ratio of mass to charge (*m/z*) of 4818.8 consistent with the calculated molecular weight of 4815 for the parent ion (M + H$^+$), $C_{228}H_{250}N_{33}O_{72}Cl_6$. The $R'_tL'_3$ species was synthesized from coupling of N$^\alpha$-acetyl-L-Lys-D-Ala-D-Ala-*tert*-butyl ester with 1,3,5-benzene tris (carbonyl chloride) and purified by reverse-phase HPLC after deprotection of the *tert*-butyl ester. ^{1}H-NMR (400 MHz, dry dimethyl-d_6 sulfoxide) δ (ppm) relative to TMS: 1.16 (d, 9 H, CHCH_3), 1.26 (d, 9 H, CHCH_3), 1.22–1.36 (m, 6 H, CH_2), 1.43–1.64 (m, 12 H, CH_2), 1.81 (s, 9 H, $COCH_3$), 3.24 (d, 6 H, CH_2NH), 4.13–4.19 (m, 6 H, COC*H*NH), 4.28 (m, 3 H, C*H*CH_3), 8.03 (d, 3 H, NH), 8.08 (d, 3 H, NH), 8.15 (d, 3 H, NH), 8.34 (s, 3 H, ArH), 8.65 (t, 3 H, NH); ESIMS exhibited an ion at *m/z* of 1148.7 consistent with the calculated *m/z* of 1147 for $C_{51}H_{79}N_{12}O_{18}$ (M + H$^+$).
21. The value of the rate constant for dissociation of the monovalent complex of vancomycin with **L** is k_{off} = 31 s^{-1} [P. H. Popieniek and R. F. Pratt, *J. Am. Chem. Soc.* **113**, 2264 (1991)].
22. A different method, ITC titration, was also used to estimate K_d^m, and yielded a slightly different value of 2.7 μM (Table 1).
23. Our analyses assume that the two intermediate species, $R'_tL'_3{\cdot}R_tV_3{\cdot}2L$ and $R'_tL'_3{\cdot}R_tV_3{\cdot}L$, are present in very small amounts at equilibrium and are thus negligible. This assumption leads to Eq. 5, which predicts a linear plot of $\theta/[R'_tL'_3]$ versus θ. The agreement of our experimental results with this prediction suggests that this assumption is valid under our experimental conditions.
24. The values of [**L**], $[R'_tL'_3]$, and θ in Eq. 5 were determined as follows: [**L**] was assumed to be constant, because **L** was in excess in the experiments; $[R'_tL'_3]$ was estimated from integration of the peaks for $R'_tL'_3$ on HPLC; θ was calculated using Eq. 4, where $[R_tV_3{\cdot}R'_tL'_3]$ was estimated from its integration, and $[R_tV_3{\cdot}3L]$ was from the integration of R_tV_3, because $R_tV_3{\cdot}3L$ dissociated to R_tV_3 on the column (*21*).
25. In a typical ITC experiment, a solution of the ligand is injected stepwise into a stirred solution of the receptor; after each injection, heat evolves because of binding. Integration of the evolved heats is a measure of the enthalpy of binding (ΔH°); analysis of the titration curve yields a value of the binding constant [T. Wiseman, S. Williston, J. F. Brandt, L.-N. Lin, *Anal. Biochem.* **179**, 131 (1989)].
26. The entropic loss of the first binding event in the trivalent complex would be expected to be larger than that of the monovalent binding of **V** to **L**, because R_tV_3 and $R'_tL'_3$ have larger sizes and more conformational freedom than **V** and **L**. The next two steps would be less entropically unfavorable than the first binding event, because they take place intramolecularly.

27. Supported by NIH grants GM 30367 (G.M.W.), GM 51559 (G.M.W.), and GM 53210 (R.M.W.). J.R. thanks Eli Lilly (1996–97) and Hoffmann–LaRoche (1997–98) for doctoral fellowships. L.I. thanks NIH for a postdoctoral fellowship.

5 January 1998; accepted 16 March 1998

An Analysis of the Origins of a Cooperative Binding Energy of Dimerization

Dudley H. Williams,* Alison J. Maguire, Wakako Tsuzuki, Martin S. Westwell

The cooperativity between binding of cell wall precursor analogs (ligands) to and antibiotic dimerization of the clinically important vancomycin group antibiotics was investigated by nuclear magnetic resonance. When dimerization was weak in the absence of a ligand, the increase in the dimerization constant in the presence of a ligand derived largely from changes associated with tightening of the dimer interface. When dimerization was strong in the absence of a ligand, the increase in the dimerization constant in the presence of a ligand derived largely from changes associated with tightening of the ligand-antibiotic interface. These results illustrate how, when a protein has a loose structure, the binding energy of another molecule to the protein can derive in part from changes occurring within the protein.

Cooperativity lies at the heart of molecular recognition, which leads to biological function (*1*). It is typically exercised when numerous weak interactions operate simultaneously. We may define an interaction between two molecules of A to give A·A (dimerization) as being cooperative with the binding of B to A if the equilibrium constant for the association of two molecules of B·A (to give B·A·A·B) is greater than that for A + A → A·A. Here, we investigate the molecular origins of such cooperativity and define a method for locating the origins of cooperative binding energy. We define the interfacial bindings in B·A and A·A as "loose" or "tight." In tight binding, the bonds that identify the individual interactions at the interface give a relatively large (perhaps near maximal) binding energy; that is, the average bond lengths are relatively short. In contrast, loose binding means that the corresponding interactions are associated with longer average bond lengths, which give an appreciably lower binding energy than that available in a tight structure. Loose interactions occur when the sum of the favorable bonding interactions (enthalpy) is sufficiently small to be counteracted by the adverse entropy of binding and when there is a relatively large amount of residual motion in the bound state (*2*).

We provide experimental evidence for the validity of the above considerations in the following sequence of steps:

1) The occurrence of loose and tight interactions, but otherwise involving a common set of weak bonds, was shown through the use of proton chemical shift changes upon association. Using the chemical shift criterion, we showed that associated structures involving one interface (B + A → B·A or A + A → A·A) tighten at that interface as the equilibrium constant for their formation increases.

D. H. Williams, Cambridge Centre for Molecular Recognition, Department of Chemistry, University of Cambridge, Lensfield Road, Cambridge CB2 1EW, UK.
A. J. Maguire, Clinical Microbiology and Public Health Laboratory, Level 6, Addenbrookes Hospital, Hills Road, Cambridge CB2 2QW, UK.
W. Tsuzuki, National Food Research Institute, Ministry of Agriculture, Forestry and Fisheries, 2-1-2 Kannondai, Tsukuba, Ibaraki, 305 Japan.
M. S. Westwell, Dyson Perrins Laboratory, University of Oxford, South Parks Road, Oxford OX1 3QY, UK.

*To whom correspondence should be addressed. E-mail: dhw1@cam.ac.uk

2) In cases in which structural tightening could occur at two different interfaces, we used the chemical shift criterion to show the extent to which it occurs at one of these interfaces. Thus, when B·A·A·B is formed from two molecules of B·A, structural tightening could occur at both the B-A (or A-B) and A-A interfaces. A chemical shift change at the A-A interface was used to determine the extent of structural tightening at this interface.

The cell wall precursor analogs (ligands) **1** to **4** (Scheme 1) bind progressively more strongly to glycopeptide antibiotics of the vancomycin group. A common feature of all these ligand-antibiotic interactions is the binding of a carboxylate anion of the ligand into a pocket of three amide NH groups of the antibiotics (Scheme 2). The binding constants (K_{lig}) of **1**, **2**, **3**, and **4** are about 10, 3×10^2, 10^5, and 10^6 M^{-1}, respectively (*3*). We recently concluded that one of the carboxylate oxygen molecules of the carboxyl group (which is common to **1** to **4**) binds more intimately to the NH w_2 (labeled in Scheme 2) of the antibiotics as K_{lig} increases (*4*, *5*). This conclusion was shown from the increasing downfield chemical shifts of w_2 in the fully bound states.

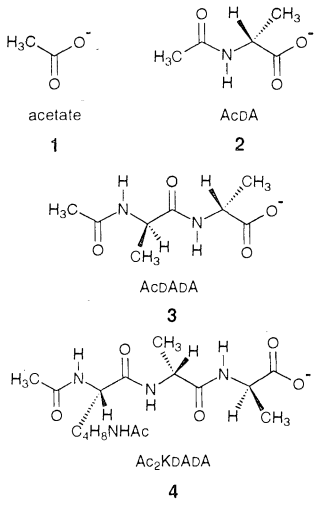

Scheme 1. Cell wall precursor analogs, which bind progressively more strongly (in the order **1**, **2**, **3**, **4**) to vancomycin group antibiotics.

Such phenomena should be general, and therefore we next sought analogous data in the dimerization of the glycopeptide antibiotics, a property that promotes their antibiotic action (*6*, *7*). The antibiotics dechlorovancomycin (**5**) (R_3 = Cl, R_4 = H), vancomycin (**6**) (R_3 = R_4 = Cl), chloroeremomycin (**7**) (R_3 = R_4 = Cl), phenylbenzylchloroeremomycin (**8**) (R_3 = R_4 = Cl), and eremomycin (**9**) (R_3 = H, R_4 = Cl) (Scheme 3) exhibit dimerization constants in the range of 10^2 to $10^{5.7}$ M^{-1}. Ristocetin-pseudoaglycone (ristocetin-Ψ; **10**) (Scheme 3), which has some different peptide side chains than **5** to **9**, has a dimerization constant of 50 M^{-1}.

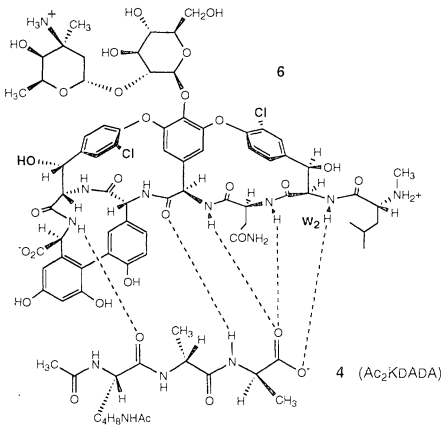

Scheme 2. The binding interface between di-*N*-acetyl-Lys-D-Ala-D-Ala (Ac_2KDADA) (**4**) and vancomycin (**6**), with the interfacial hydrogen bonds represented by broken lines and with the monitored proton w_2 indicated.

Despite the large variation in the dimerization constants, the dimer interfaces for the six glycopeptide antibiotic dimers discussed here all contain the common arrangement of four interfacial amide-amide hydrogen bonds (Scheme 4) (*6*, *8*–*10*). In particular, the proton x_4 (Scheme 4) at the dimer interface suffers a relatively large downfield shift upon dimerization. The extent of this downfield shift ($\Delta\delta x_4^{lim}$) was used to reach conclusions with regard to the looseness or tightness of the dimer interfacial structure as a function of the dimerization constant (*5*). The change in chemical shift of x_4 ($\Delta\delta x_4^{lim}$) in passing from monomer to dimer structure is much larger in the case of the formation of a strongly bound dimer than for that of a weakly bound dimer (Table 1 and Fig. 1A). We emphasize that the nuclear magnetic resonance (NMR) experiments gave $\Delta\delta x_4^{lim}$ values that corresponded to the difference in chemical shift between fully monomeric and fully dimeric species ($\Delta\delta x_4^{lim}$) (*5*) and that the smaller $\Delta\delta x_4^{lim}$ values observed for the more weakly dimerizing antibiotics therefore did not correspond to only partially dimerized antibiotics. In summary, the two sets of data indicate that, in the binding of a ligand to an antibiotic or in the dimerization of the antibiotics, the entities come into more intimate contact as the equilibrium constants for the respective associations increase.

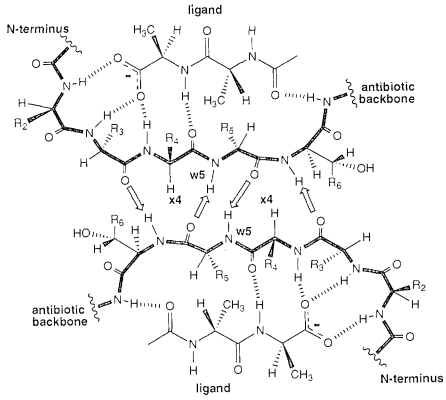

Scheme 4. Structure of the antibiotic dimer with its peptide backbone indicated in bold, shown here with acetyl-D-Ala-D-Ala (ligand) bound in each binding site. Hydrogen bonds at the dimer interface are indicated by open arrows, and those at the ligand-antibiotic interface are indicated by dashed lines. N-terminus, NH_2-terminus.

The free energy ΔG values for the conversions of the ligand-bound monomers of **5** to **10** to ligand-bound dimers show that, in all cases, the dimerization is cooperative with ligand binding (Table 1). The corresponding changes in the chemical shift of x_4 for **5** to **10** for the conversion of ligand-

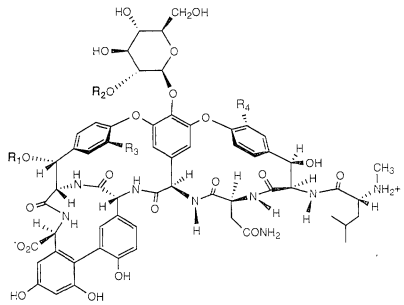

	R_1	R_2
5 dechlorovancomycin	H	vancosamine
6 vancomycin	H	vancosamine
7 chloroeremomycin	4-*epi*-vancosamine	4-*epi*-vancosamine
8 phenylbenzylchloro-eremomycin	4-*epi*-vancosamine	*p*-phenylbenzyl-4-*epi*-vancosamine
9 eremomycin	4-*epi*-vancosamine	4-*epi*-vancosamine

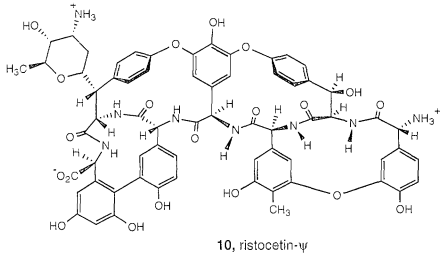

Scheme 3. Structures of the glycopeptide antibiotics (with the nature of the R_3 and R_4 groups indicated in the text), which have dimerization constants over the range of about 10^2 to 10^6 M^{-1}.

bound monomers to ligand-bound dimers suggest that when dimerization is strong even in the absence of a ligand (**8** and **9**), the cooperative binding expressed in the presence of a ligand causes little tightening at the dimer interface (Table 1); that is, there is little increase in $\Delta\delta x_4^{lim}$ caused by the presence of a ligand (compare Fig. 1, A and B) (*11–13*).

If the dimer interface is loose in the absence of a ligand [small value of the dimer binding constant K_{dim} (and of $-\Delta G_{dim}$)], an important contribution to the increase in K_{dim} (and of $-\Delta G_{dim}$) in the presence of a ligand will come from changes associated with the tightening of the dimer interface (increase in limiting chemical shift of x_4). Conversely, if the dimer interface is tight even in the absence of a ligand (large values of K_{dim} and $-\Delta G_{dim}$), then the major portion of the favorable free energy change that causes an increase in K_{dim} in the presence of a ligand should actually come from changes associated with the tightening of the ligand-antibiotic interface, and there should be little accompanying change in the limiting chemical shift of x_4. The way in which the cooperative free energy of dimerization can be partitioned into changes associated with the dimer interface or with the ligand-antibiotic interface is indicated by sets of hypothetical points in Fig. 2A. The expectation is that a weakly dimerizing compound will largely exercise cooperativity by tightening the dimer interface (arrows joining open and filled circles for the same antibiotic at a shallow angle to the horizontal; for example, W in Fig. 2A). In contrast, a strongly dimerizing compound will largely exercise cooperativity by tightening the interface with the ligand (arrows joining open and closed circles for the same antibiotic at a very steep angle to the horizontal; for example, Z in Fig. 2A).

The experimental data (Fig. 3) follow the postulated expectation from Fig. 2 remarkably closely. The weakly dimerizing antibiotics ristocetin-Ψ (**10**) and dechlorovancomycin (**5**) dimerized more strongly in the presence of di-*N*-acetyl-Lys-D-Ala-D-Ala than in its absence essentially because the free energy of binding associated with changes at the dimerization interface is more favorable. The more strongly dimerizing antibiotics chloroeremomycin (**7**), phenylbenzylchloroeremomycin (**8**), and eremomycin (**9**) dimerized more strongly in the presence of di-*N*-acetyl-Lys-D-Ala-D-Ala than in its absence largely because the free energy of binding associated with changes at the antibiotic-ligand interface is more favorable in B·A·A·B than in B·A. There was little change in the free energy of binding associated with changes at the dimer interface. The behavior of vancomycin (**6**) was between these two extremes.

Our findings have implications for the study of protein-protein interactions and for drug design. In both areas, it is common practice to seek the origins of binding affinity at the interface formed between the associating entities (*14*, *15*). Our data (Fig. 3) show that when the antibiotics **8** and **9** dimerize more strongly in the presence of a ligand (relative to its absence), the increase in the equilibrium constant for dimerization arises largely from changes associated with the tightening of the interaction between the ligand and the antibiotic. By analogy, when proteins (or, more specifically, recep-

Table 1. Chemical shifts of the proton x_4 in monomeric and dimeric forms of the glycopeptide antibiotics **5** to **10** [both in the presence and absence of di-*N*-acetyl-Lys-D-Ala-D-Ala (Ac_2KDADA)]. δx_{4mon}^{lim} is the chemical shift of the proton x_4 in the antibiotic monomer, δx_{4dim}^{lim} is the chemical shift of x_4 in the fully bound dimer, and $\Delta\delta x_4^{lim}$ is the difference between these chemical shifts. ΔG_{dim} is the free energy change for the formation of a dimer from a monomer.

	δx_{4mon}^{lim} (ppm)	δx_{4dim}^{lim} (ppm)	$\Delta\delta x_4^{lim}$ (ppm)	$-\Delta G_{dim}$ (kJ mol^{-1})
5	5.72	6.27	0.55	11.9
5 + Ac_2KDADA	5.76	6.49	0.73	16.9
6	5.68	6.38	0.70	14.8
6 + Ac_2KDADA	5.82	6.57	0.75	20.1
7	5.69	6.47	0.78	24.0
7 + Ac_2KDADA	5.67	6.48	0.81	35.9
8	5.66	6.49	0.83	30.8
8 + Ac_2KDADA	5.67	6.51	0.84	42.7
9	5.68	6.46, 6.56*	0.83	32.1
9 + Ac_2KDADA	5.67	6.52	0.85	43.9
10	5.42	5.90	0.48	9.7
10 + Ac_2KDADA	5.58	6.23	0.65	15.8

*When x_4 showed two chemical shifts because of asymmetry in the dimer, the average of these two values was used in deriving $\Delta\delta x_4^{lim}$.

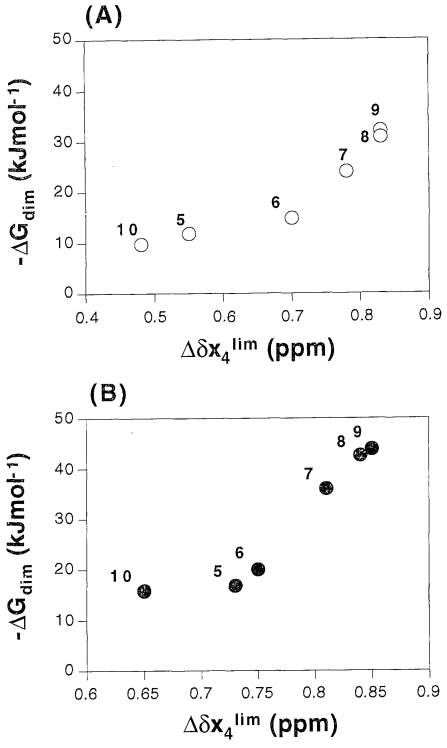

Fig. 1. (**A**) Plot of $-\Delta G_{dim}$ versus $\Delta\delta x_4^{lim}$ for the free antibiotics **5** to **10**. [Modified from (*5*) and reproduced with permission of *Current Biology Limited*.] (**B**) Plot of $-\Delta G_{dim}$ versus $\Delta\delta x_4^{lim}$ for the antibiotic–di-*N*-acetyl-Lys-D-Ala-D-Ala complexes for **5** to **10**.

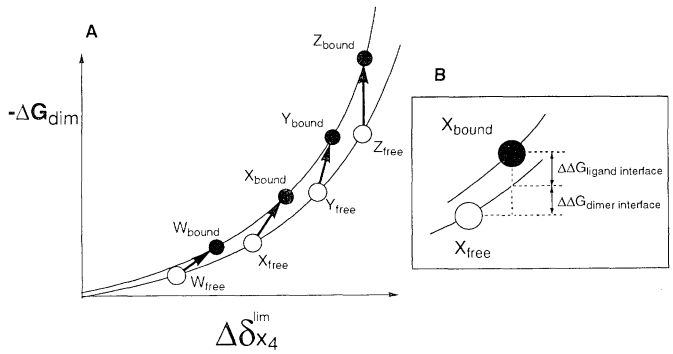

Fig. 2. (**A**) Plot of $-\Delta G_{dim}$ versus $\Delta\delta x_4^{lim}$ for hypothetical data points for free antibiotics W, X, Y, and Z (open circles) and the same set of four antibiotics when dimerizing as antibiotic-ligand complexes (filled circles). The arrows connect the hypothetical points for a given antibiotic, and the series of antibiotics W, X, Y, and Z have increasing dimerization constants. (**B**) Because the free energy of dimerization associated with changes at the dimer interface is defined by the curve connecting the points (open circles) for the dimerization of antibiotic alone, the extent to which the filled circle lies vertically above this curve gives the free energy of dimerization associated with changes in the ligand-antibiotic interfaces.

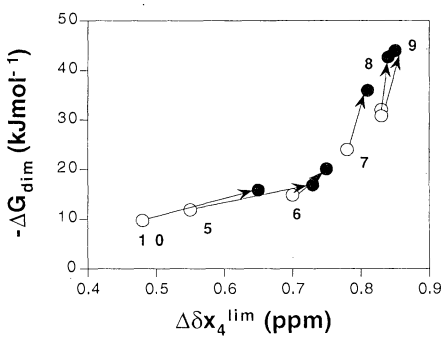

Fig. 3. Combined plot of $-\Delta G_{dim}$ versus $\Delta\delta x_4^{lim}$ for free (open circles) and ligand-bound (filled circles) antibiotics **5** to **10**. For any one antibiotic, arrows represent changes occurring upon ligand binding.

tors) have loose structures before binding another protein (or in the specific case of a receptor, its natural ligand or a drug), then a portion of the binding affinity can be derived by tightening of the internal structures of the proteins in the resulting bound state. Given this possibility, the thermodynamic parameters for protein-protein associations, which are perplexing when analyzed in terms of interfacial interactions (*14*), can be seen to have much more complex origins. The findings may also be relevant to transmembrane signal transduction, most obviously when signal activation is coincident with receptor dimerization (*16*). Suppose a ligand binds strongly to the monomeric form of a receptor (which itself dimerizes weakly in the absence of a ligand) and binds cooperatively to the dimeric form of the receptor. Such a system is well constituted to produce a tightening of the structure of the receptor at its dimer interface and hence to assist in ligand-induced changes in geometry (even without obvious allosteric changes) at points remote from ligand binding.

REFERENCES AND NOTES

1. L. Stryer, *Biochemistry* (Freeman, New York, ed. 3, 1988), pp. 82, 154–156, 234, 240, 267, and 290.
2. D. H. Williams and M. S. Westwell, *Chem. Biol.* **3**, 6953 (1996).
3. D. H. Williams *et al.*, *J. Am. Chem. Soc.* **113**, 7020 (1991).
4. M. S. Searle *et al.*, *J. Chem. Soc. Perkin Trans. 1* **X**, 2781 (1996).
5. D. H. Williams *et al.*, *Chem. Biol.* **4**, 507 (1997).
6. J. P. Mackay *et al.*, *J. Am Chem. Soc.* **116**, 4581 (1994).
7. D. A. Beauregard, D. H. Williams, M. N. Gwynn, D. J. C. Knowles, *Antimicrob. Agents Chemother.* **39**, 781 (1995).
8. G. M. Sheldrick, E. Paulus, L. Vertesy, F. Hahn, *Acta Crystallogr. B* **51**, 89 (1995).
9. M. Schafer, T. R. Schneider, G. M. Sheldrick, *Structure* **4**, 1509 (1996).
10. P. J. Loll, A. E. Bevivino, B. D. Korty, P. H. Axelson, *J. Am. Chem. Soc.* **119**, 1516 (1997).
11. Before we recorded the NMR spectra, we lyophilized the glycopeptides twice from D_2O. All samples were prepared at pD 3.7 by adjustment with NaOD and CD_3CO_2D or DCl. All pD sample readings were measured with a Corning pH meter equipped with a combination glass electrode, and no corrections were made for an isotope effect. NMR spectra were recorded on Bruker DRX500 spectrometers, and one-dimensional (1D) and two-dimensional (2D) spectra were recorded with 16,000 or 8000 data points, respectively. Chemical shifts were measured with respect to internal sodium 3-trimethylsilyl-2,2,3,3-d_4-propionate at 300 K.
12. When monomer and dimer forms of the antibiotic were in fast exchange on the NMR time scale, δx_4 was typically followed in 1D spectra obtained over a concentration range (3 mM to 25 or 100 mM, depending on the antibiotic), and monomer and dimer chemical shifts obtained from curve fitting (Simplex least squares curve-fitting program) of the data were extrapolated to infinitely dilute and infinitely large concentrations. When peak overlap precluded the following of x_4 in 1D spectra, appropriate cross peaks in 2D spectra were used. In the cases in which a large dimerization constant resulted in slow exchange between the monomer and dimer on the NMR time scale, the x_4 signals from the monomer and dimer were correlated by preirradiation of the dimer signal, which resulted in a reduction in intensity of the signal due to x_4 in the monomer. For these antibiotics, appearance of the monomer signal could be followed in the 5 mM to 10 μM concentration range. The signal from x_4 in the monomer of **8** and **9** in the presence of di-*N*-acetyl-Lys-D-Ala-D-Ala could not be unambiguously assigned because of overlap with other signals in this region and the need for exceptionally low concentrations. The antibiotics **7**, **8**, and **9** have the same x_4 chemical shift for the monomer in the absence of di-*N*-acetyl-Lys-D-Ala-D-Ala [±0.02 parts per million (ppm)]. Considering the structural similarities of **7**, **8**, and **9**, it was considered reasonable to take the x_4 chemical shift for the monomers of **8** and **9** bound to di-*N*-acetyl-Lys-D-Ala-D-Ala as equal to that for **7**.
13. For antibiotics in which the monomer and dimer species were in fast exchange on the NMR time scale, the chemical shift of x_4 was followed at different antibiotic concentrations. From a plot of δx_4 versus concentration, the dimerization constants and limiting chemical shifts could be calculated (*6*). For antibiotics in which the monomer and dimer species were in slow exchange on the NMR time scale, at sufficiently low concentrations of antibiotic (10 to 100 μM), both monomer and dimer states were populated. Integration of appropriate peaks yielded K_{dim}. For **7**, **8**, and **9** in the presence of a ligand, K_{dim} was calculated from the rate of exchange (H → D) of the NH (w_5, see **11**) at the antibiotic interface (*6*) in comparison with the rate of exchange of this same NH in **7** to **9** (in the absence of a ligand), where K_{dim} is known.
14. For a recent review of protein-protein interactions, see W. E. Stites, *Chem. Rev.* **97**, 1233 (1997).
15. H.-J. Bohm, *J. Comput.-Aided Mol. Des.* **8**, 243 (1994).
16. F. Canals, *Biochemistry* **31**, 4501 (1992).

17. We thank BBSRC for financial support. A.J.M. gratefully acknowledges SmithKline Beecham, and M.S.W. thanks GlaxoWellcome Research and Lincoln College, Oxford. W.T. thanks the National Institute of Food Research, Ministry of Agriculture, Food, and Fisheries, Japan. Vancomycin, dechlorovancomycin (LY223997), chloroeremomycin (LY264826), and phenylbenzylchloroeremomycin (LY307599) were generously donated by Eli Lilly (Indianapolis, IN). Eremomycin was a gift from SmithKline Beecham (Harlow, UK).

20 January 1998; accepted 10 March 1998

Elucidation of the Chain Conformation in a Glassy Polyester, PET, by Two-Dimensional NMR

K. Schmidt-Rohr,* W. Hu, N. Zumbulyadis

The chain conformation of glassy poly(ethylene terephthalate) (PET) was characterized by two-dimensional double-quantum nuclear magnetic resonance (NMR). In amorphous carbon-13–labeled PET, the statistics of the O–$^{13}CH_2$–$^{13}CH_2$–O torsion angle were determined, on the basis of the distinct shapes of the two-dimensional NMR patterns of trans and gauche conformations. In crystalline PET, the trans content is 100 percent, but in the amorphous PET it is only 14 percent (±5 percent). An average gauche torsion angle of 70 degrees (±9 degrees) was obtained. Implications for materials properties of polyesters are discussed.

PET (Fig. 1) and related aromatic polyesters find widespread uses in tough, transparent packaging materials with good barrier properties, in polyester fibers, and in thin films for photographic or magnetic-tape applications, which represent multibillion dollar industries (*1*). The degree of crystallinity can vary from 0 to 50%, and noncrystalline glassy polyesters can be obtained by quenching from the melt, which produces transparent films. To understand details of the materials properties of amorphous and semicrystalline polyesters, such as glass-transition and melting temperatures, crystallization rates, maximum crystallinities, or gas-barrier properties, knowledge of their microscopic structure is required. Although the chemical and the crystal structures of PET are well known (Fig. 1) (*2–4*), the chain conformations in the amorphous state are poorly characterized. The torsion around the OC–CO single bond (Fig. 1) is the major degree of freedom; bond lengths

K. Schmidt-Rohr and W. Hu, Department of Polymer Science and Engineering, University of Massachusetts, Amherst, MA 01003, USA.
N. Zumbulyadis, Imaging Research and Advanced Development, Eastman Kodak Company, Rochester, NY 14650–2132, USA.

*To whom correspondence should be addressed.